

Unifying individual and metapopulation scales with stochastic population models: the effect of climate and competition on tree range limits

WILLIAN VIEIRA^{*1} AND DOMINIQUE GRAVEL¹

¹DÉPARTEMENT DE BIOLOGIE, UNIVERSITÉ DE SHERBROOKE, SHERBROOKE, QUÉBEC, CANADA

Running title: Unifying scales with stochastic population models

Supporting information: Additional supporting information can be found [here](#).

Acknowledgments: We thank nice people

Data availability: All the code and data used to reproduce the analysis, figure and manuscript are stored as a research compendium at https://github.com/willviera/ms_forest-suitable-probability).

Funding: This research was supported by the BIOS² NSERC CREATE program.

Conflicts of interest: The authors declare no conflict of interest.

Abstract

^{*}Corresponding author: willian.vieira@usherbrooke.ca

Despite recent calls to use demographic range models to scale the effect of individual dynamics in setting range limits, there is a growing body of evidence showing that tree species' performance is not correlated with their distribution. In this study, we ask whether the challenge in predicting species distribution from demographic rates stems from overlooking the inherent variability of forest systems and the underlying uncertainty of forest models. We use a stochastic Integral Projection Model to predict species-level intrinsic population growth (λ) for 31 eastern North American tree species. We introduce a novel metric for species-level performance called local suitable probability, which captures observed spatiotemporal stochasticity in climate and competition while accommodating model uncertainty. Our focus is on investigating how suitable probability changes across the cold-to-hot species range distribution over the mean annual temperature gradient. Our findings reveal a consistent, nearly linear decline in suitable probability from the cold to hot borders across the species. This shift in suitable probability from the center towards the cold and hot borders is primarily driven by climate rather than competition. These results, supported by a novel approach accounting for uncertainty, enhance our understanding of the nuanced interplay between climate and competition across species ranges. We conclude by proposing a novel theory that uses the local suitable probability to establish a link between individual demographic rates and metapopulation dynamics.

Keywords: Integral Projection Models, Species distribution, Individual variability, Environmental stochasticity, Forest demography

1 Introduction

Climate warming poses a significant challenge for several species, particularly for trees that struggle to follow temperature warming and moving ranges (Sittaro et al. 2017). It is imperative to untangle the mechanisms governing their range limits to forecast how they will respond to climate change. The niche theory predicts that a species will be present in suitable environmental conditions that allow the

species to have a positive growth rate (Hutchinson 1957). From this theory, we can define the geographic distribution of a species as a manifestation of individual demographic rates, such as growth, survival, and recruitment (Holt 2009). By assuming these demographic rates change with the environment, we can predict a species' range limits based on its individuals' performance (Maguire Jr 1973, Holt 2009).

Biotic interaction is undoubtedly an essential driver of demographic rates and, thereby, should also range limits. A recent theoretical framework based on the coexistence theory has been proposed to assess how biotic interactions can scale up to affect range limits (Godsoe et al. 2017). Formally, this framework evaluates the intrinsic population growth rate when the focal species is rare (Chesson 2000), both in scenarios where there is no competition (fundamental niche) and when competitive species reach equilibrium (realized niche). Numerous studies have explored the influence of climate and competition on the distribution of forest trees across their ranges. For instance, Ettinger and HilleRisLambers (2017) observed in field experiments that neighboring competition constrained individual performance within the range but facilitated better performance outside the range. Using a dynamic forest model, Scherrer et al. (2020) showed how slow demographic rates and negative competition reduce the uphill migration rate of 16 tree species. Despite this evidence, the application of this framework to predict the geographic distribution of species based on demographic rates often reveals weak correlations between the performance of tree species and their distribution (McGill 2012, Csergo et al. 2017, Bohnert and Diez 2020, Le Squin et al. 2021, Midolo et al. 2021, Guyennon et al. 2023, Thuiller et al. 2014).

One possible explanation for such discrepancy between demographic rates and species distribution is the common practice of assessing performance under average conditions and pointwise estimations, neglecting the associated uncertainty in these estimates. In ecological models, the uncertainty in estimation arises from three distinct sources. The first source involves measurement errors, a factor often neglected in ecological models (Damgaard 2020). The second is process uncertainty linked to model (mis)specification (Harwood and Stokes 2003). Even with a well-defined model and precise data, models must also consider parameter uncertainty (Cressie et al. 2009, Shoemaker et al. 2020).

Beyond data and model uncertainty, variability in demographic rates and subsequently in the population growth rate (λ) arises from two primary sources (van Daalen and Caswell 2020). The first is attributed to demographic and environmental stochasticity, where individuals exposed to identical conditions may

74 exhibit different responses simply by chance (Caswell 2009). The second source of variability arises from
75 heterogeneity encountered at various scales. These differences can manifest between individual stages
76 that motivated the development of structured population models (Lewis 1942, Leslie 1945), and can
77 promote high species diversity in forest trees (Clark 2010). Another source of heterogeneity arises from
78 large-scale differences in neighboring patches, often described by the metapopulation theory (Levins
79 1969). This theory posits that the dynamics of occupied and empty patches in a landscape are driven
80 by colonization and extinction processes. This theory posits that the dynamics of occupied and empty
81 patches in a landscape are driven by colonization and extinction processes. Building on this theory,
82 Talluto et al. (2017) used patch variability to derive colonization and extinction rates of eastern North
83 American trees, revealing their distribution to be out of equilibrium with climate. Therefore, while this
84 result advances our understanding of the mechanisms governing large-scale tree distributions, there
85 remains a need to reconcile it with local demographic dynamics, given that colonization and extinction
86 processes ultimately manifest from demographic rates.

87 Theory predicts that the uncertainty arising from stochastic and heterogenous processes may lead to
88 divergent outcomes in λ . Demographic and environmental stochasticity may increase the uncertainty
89 in λ , consequently increasing the extinction risk, particularly for populations with low performance or
90 low density (Holt et al. 2005, Gravel et al. 2011). For instance, demographic stochasticity increased
91 the extinction risk of European forest trees at the hot edge of their distribution (Guyennon et al.
92 2023). On the other hand, spatial heterogeneity has been described as a buffering process against the
93 stochasticity in demographic rates, thereby increasing population persistence (Milles et al. 2023). This
94 is particularly relevant in nonlinear models, where Jensen’s inequality predicts - for convex response
95 functions - that higher demographic and environmental stochasticity increases the average population
96 growth rate (Koons et al. 2009). Furthermore, demographic and environmental stochasticity influence
97 abundance variation, indirectly impacting λ through density-dependence (May et al. 1978, Terry et
98 al. 2022). A comprehensive understanding of the response of forest trees to climate change requires
99 incorporating the multiple sources of variability arising from spatio-temporal variation and parameter
100 uncertainty.

101 Here, we use a stochastic Integral Projection Model (IPM) to predict species-level intrinsic population
102 growth (λ) for 31 eastern North American tree species. The IPM integrates the growth, survival, and

recruitment demographic rates, which vary in response to climate and competition. By fitting each demographic rate using non-linear hierarchical Bayesian models, we capture parameter uncertainty at both the individual and local population scales. Additionally, our model naturally accommodates observed spatio-temporal stochasticity in climate and competition. Then, rather than ignoring these sources of variability, we embrace them into λ by defining species performance through a probabilistic framework. Specifically, we introduce a novel metric called **local suitable probability**, derived from the average population growth rate and its associated variability. This metric determines the probability of a positive population growth rate for a species under specific climate and competition conditions.

Our analysis is as follows. First, we used the IPM to predict species-specific λ at the plot level under two conditions: without (fundamental niche) and with (realized niche) heterospecific competition. By replicating this calculation 100 times across all observed plots from the same species, we can assess the variability of λ arising from both spatio-temporal stochasticity in the climate and competition and model uncertainty. As this variable λ changes across space, we used these observations to model how the species' local suitable probability changes across the mean annual temperature. Specifically, we ask how climate and competition affect each species' local suitable probability. Then, we investigated how a species' local suitable probability changes from the center of its distribution toward the cold and hot borders. Finally, we disentangle the relative impacts of climate and competition in changing suitable probability from the center to the borders. We conclude by discussing a novel theory that uses the local suitable probability to establish a link between individual demographic rates and metapopulation dynamics.

2 Methods

2.1 Population model, demographic components, and uncertainty structure

We use an Integral Projection Model (IPM) to predict the intrinsic population growth rate (λ) as a function of climate and competition. An IPM is a powerful modeling approach that allows a full representation of all sources of variability in demography. The IPM serves as a mathematical formulation

describing the dynamics of a continuous trait distribution (z) within a population over discrete time steps:

$$n(z', t + 1) = \int_L^U K(z', z, X, \theta) n(z, t) dz \quad (1)$$

In our case, the trait z is defined as the tree's diameter at breast height (dbh), constrained between the limits L and U . The continuous distribution $n(\cdot)$ of dbh z of a population at time t transitions to the next time step using a projection kernel (K). The kernel K , with parameters θ and covariates X that are time dependent, comprises three demographic submodels:

$$k(z', z, \theta) = [Growth(z', z, X, \theta) \times Survival(z, X, \theta)] + Recruitment(z, X, \theta) \quad (2)$$

The growth model assesses the probability of an individual of size z at time t transitioning to size z' at time $t + 1$. The survival model determines the probability of an individual with size z at time t surviving to the next time step. Lastly, the recruitment model determines the number of new individuals entering the population at each time step as a function of total density z . The kernel K has the same function of the population growth rate r in a population model, where multiplying the population distribution $n(z, t)$ with K gives the population distribution at the next time step $n(z', t + 1)$. Its advantage in propagating uncertainty is that, instead of having a matrix with fixed parameters determining the transition rate of population individuals over time, it uses a probability distribution with uncertainty derived from the demographic models to project individuals over time.

With the defined K , we can estimate the intrinsic population growth rate for a determined set of conditions from the covariates X and sampled parameters from the posterior distribution θ . Specifically, we discretize the continuous kernel K using the mid-point rule (Ellner et al. 2016) and estimate the intrinsic population growth rate using the dominant eigenvalue of the discretized K . This approach is a local approximation of the population growth rate at the initial time steps.

A detailed description of the data and model development is available in Chapter 2. In summary, we evaluated non-linear statistical models to formulate the growth, survival, and recruitment components

151 of the IPM, along with their uncertainty. Each demographic sub-model varies as a function of the
 152 mean annual temperature, mean annual precipitation, and stand basal area of larger individuals. Each
 153 model's parameters (θ) are species-specific, as each model is fitted separately for each species. Both
 154 climate variables influence each demographic model through an unimodal link function, where each
 155 model exhibits an optimal climate and niche breadth for temperature and precipitation. Additionally,
 156 density dependence is integrated based on the plot's total basal area of larger individuals. Stand density
 157 affects growth and survival through a linear model, in which two parameters determine the strength of
 158 interaction from conspecific and heterospecific (all species combined) competition. For the recruitment
 159 model, the annual ingrowth rate is modulated by conspecific stand basal area, using an unimodal
 160 function to account for both the positive effect of seed source and the negative effect of conspecific
 161 competition. Furthermore, the annual survival rate of potential ingrowth individuals decreases linearly
 162 with the stand density of heterospecific individuals. Finally, the intercept of each growth, survival, and
 163 recruitment model incorporates plot-level random effects to control for the variance shared within the
 164 plot-year observations.

165 We use two open inventory datasets from eastern North America: the Forest Inventory and Analysis
 166 (FIA) dataset in the United States (O'Connell et al. 2007) and the permanent plots of forest inventory
 167 program for Québec (Ministere des Ressources Naturelles 2016). These inventories, with multiple
 168 individual measurements over time and space, allow us to use the transition information between
 169 measurement years for predicting growth, survival, and recruitment rates. We selected the 31 most
 170 abundant species, comprising 9 conifer species and 21 hardwood species, well-dispersed across shade
 171 tolerance and successional status (Supplementary Material 1). These species are well distributed across
 172 the eastern North American gradient and the sampling area covers cold and hot range limits for most
 173 species.

174 **2.2 Extracting local suitability probability**

175 We estimate λ at the local population scale, specifically at the plot level in our study. Within a given
 176 geographic location, such as a specific latitude where several plots are located, the variance of λ among
 177 those plots arises from spatio-temporal variations in both climate and competition covariates. For
 178 instance, climate stochasticity introduces noise in annual temperature and precipitation, leading to

environmental variation. Similarly, even with identical climate conditions, two locations can exhibit different community abundance and composition, resulting in variability in the strength of competition. Beyond these spatio-temporal environmentally-induced variations, λ can still vary due to the other sources of uncertainty discussed above.

We track demographic model uncertainty at two complementary scales: individual and plot levels. At the individual level, plots with the same climate and competition conditions may have different λ values due to the uncertainty in the demographic sub-models. Similarly, even with the same environmental conditions and averaged parameter values (eliminating demographic uncertainty at the individual level), two plots can still yield different λ values due to the spatial uncertainty of each demographic model assigned among plots. Therefore, variability in the population growth rate can arise from spatio-temporal variations in both the environment and the parameters.

Given these different sources of variability in λ , we define the suitable probability as the area under the distribution for $\lambda \geq 1$. To estimate this, we first determine the cumulative distribution function, $F(x)$, from the generic probability density function, $\lambda = f(t)$, as follows:

$$F_{\lambda}(x) = P(\lambda \leq x) = \int_{-\infty}^x f(t)dt \quad (3)$$

This function represents the cumulative distribution from $-\infty$ to x . Subsequently, we define the suitable probability (Λ) as the complement of the cumulative distribution function for $x = 1$:

$$\Lambda = 1 - F_{\lambda}(1) \quad (4)$$

2.3 Modeling suitable probability

We can evaluate the suitable probability of a species at various scales, ranging from a single local plot up to several plots in a region. At the plot level, sources of variability in λ stem from parameter uncertainty, individual heterogeneity, and temporal variability in climate and competition. When considering multiple plots simultaneously, we can additionally account for spatial variability in climate

200 and competition, along with spatial uncertainty in plot-level parameters.

201 Apart from parameter uncertainty at the individual level, all other sources of variability exhibit spatial
202 dependence. This implies that environmental variability (from climate, competition, or both) and
203 parameter uncertainty at the plot level can vary based on their spatial location. For instance, plots at
204 the border of the species distribution may experience more temperature variability than those at the
205 center. Additionally, plot-level parameter uncertainty can be spatially clustered, capturing potential
206 features of demographic variability beyond the climatic and competition covariates, such as historical
207 factors or local edaphic conditions.

208 Given that variability can be spatially dependent, we can model how suitable probability changes across
209 the species' range distribution, considering both fixed climate and competition effects and the underlying
210 spatio-temporal variability. We are particularly interested in how suitable probability changes from the
211 center toward the cold and hot ranges. For that, we categorized all species' plot-year observations based
212 on the gradient of mean annual temperature (MAT), divided into cold and hot ranges using the MAT
213 centroid among all plots for the species ($\frac{\max(MAT)+\min(MAT)}{2}$). For instance, if a species is observed
214 within the 4-10°C gradient of MAT, the plots with MAT below 7°C are classified as cold, while the
215 others are classified as hot. We chose to use MAT instead of latitude because we are interested in the
216 species' climatic niche, although the two variables are highly correlated.

217 We assessed suitable probability separately for the cold and hot ranges, employing a linear model to
218 determine the relationship between λ and MAT. The spatio-temporal variability of λ arising from
219 environmental stochasticity and parameter uncertainty influences the variance of the linear model. As
220 this variance may change depending on the range position, we introduce a submodel for the variance of
221 the linear model to be dependent on MAT. To accommodate potential asymmetry in this variance, we
222 use a Skew Normal Distribution (*SN*) incorporating an additional parameter (α) that can introduce
223 right or left-skewed tails to the variance:

$$\log(\lambda) \sim SN(\xi, \omega, \alpha)$$

$$\xi = \beta_{1,\xi} \times MAT + \beta_{0,\xi} \tag{5}$$

$$\omega = e^{\beta_{1,\omega} \times MAT + \beta_{0,\omega}}$$

Here, ξ is the location parameter or the λ average, and ω is the scale representing the variance around the mean.

2.3.1 Simulations

We computed λ for each species based on the plot-year observations in the dataset, considering both environmentally induced variability and parameter uncertainty. For every observed species-plot-year combination, we incorporated temporal stochasticity in climate conditions by using the mean and standard deviation of mean annual temperature and precipitation calculated from the years between measurements. For instance, in the case of a plot observed twice, we calculated λ for the second observation with climate conditions drawn randomly from a normal distribution with mean and standard deviation defined from climate observations within the year interval. Similarly, temporal stochasticity in competition arises from variation in abundance and composition between measured years. By iteratively performing this calculation, drawing parameter values randomly from the posterior distribution, we introduced demographic uncertainty at the individual level. For each species-plot-year measurement, we replicated the calculation of λ 100 times. By applying this approach across all plots, we naturally incorporate spatial variation in climate and competition conditions and spatial uncertainty in plot-level parameters.

For each species-plot-year-replication combination, we calculated λ under two simulated conditions. The first scenario excludes competition in order to evaluate the fundamental niche, with heterospecific competition set at zero and conspecific total population size (N) set at 0.1. This simulation is used to assess the fundamental niche. The second scenario is used to evaluate the invasion growth rate with residents (the realized niche), with an evaluation of the population growth rate when the focal species is rare ($N = 0.1$) and heterospecific competition is set to the observed abundance of the competitive

species. This condition simulated the population growth rate under the realized niche.

We then fitted a linear model of λ for each species-plot-year-replication as a function of the mean annual temperature gradient. Species-specific linear models were evaluated for the hot and cold ranges using the Hamiltonian Monte Carlo (HMC) algorithm via the Stan software (version 2.30.1 Team and Others 2022) and the `cmdstandr` R package (version 0.5.3 Gabry et al. 2023). We used a sample of 5000 plots for each species to fit the model. This sample was necessary only for 6 out of the 31 species.

We leveraged the posterior distribution to estimate the suitable probability of a species for any value of MAT under fundamental or realized niches for the cold and hot ranges. Specifically, we estimated suitable probability under four different MAT conditions encountered by the species: at the border and the center of each cold and hot range. We defined the border of the cold range as the minimum observed MAT for the focal species in the dataset, while the hot range was defined as the maximum observed MAT. The center location is defined as the centroid of MAT for the focal species. Although the center location has the same MAT for the cold and hot ranges, both are retained because the model is fitted separately for the cold and hot ranges. Finally, we estimated suitable probability for each location under no competition (fundamental niche) and heterospecific competition (realized niche) conditions, using the empirical cumulative distribution function over 1000 predictive draws.

The code for the computation of each plot-year λ is available at https://github.com/willvieira/forest-IPM/tree/master/simulations/lambda_plot, and the code to model the linear model is at https://github.com/willvieira/forest-IPM/tree/master/simulations/model_lambdaPlot/.

3 Results

3.0.1 Model fit

We first analyzed how the local population growth rate (λ) and its variability change across the cold and hot ranges (Equation 5). An example is provided at Figure 1 with the observed distribution of λ and the fit of the underlying model on the mean annual temperature gradient for balsam fir, *Abies balsamea*. Each point represents a plot-year-replication encompassing the complete spatio-temporal sources of variability arising from the stochastic environment and parameter uncertainty. The black line

272 represents the fitted model of how λ changes with MAT, and the envelopes depict the 90th quantiles
 273 of model distribution. From this uncertainty, we can deduce the suitable probability. This example
 274 shows that the mean and variance of λ decrease towards the cold border, while it does not vary much
 275 towards the hot border. By comparing the model under heterospecific competition with that without
 276 competition for the cold range, we observed that while their average is similar, the uncertainty of the
 277 model under heterospecific competition shifted downwards (Figure 1, bottom left).

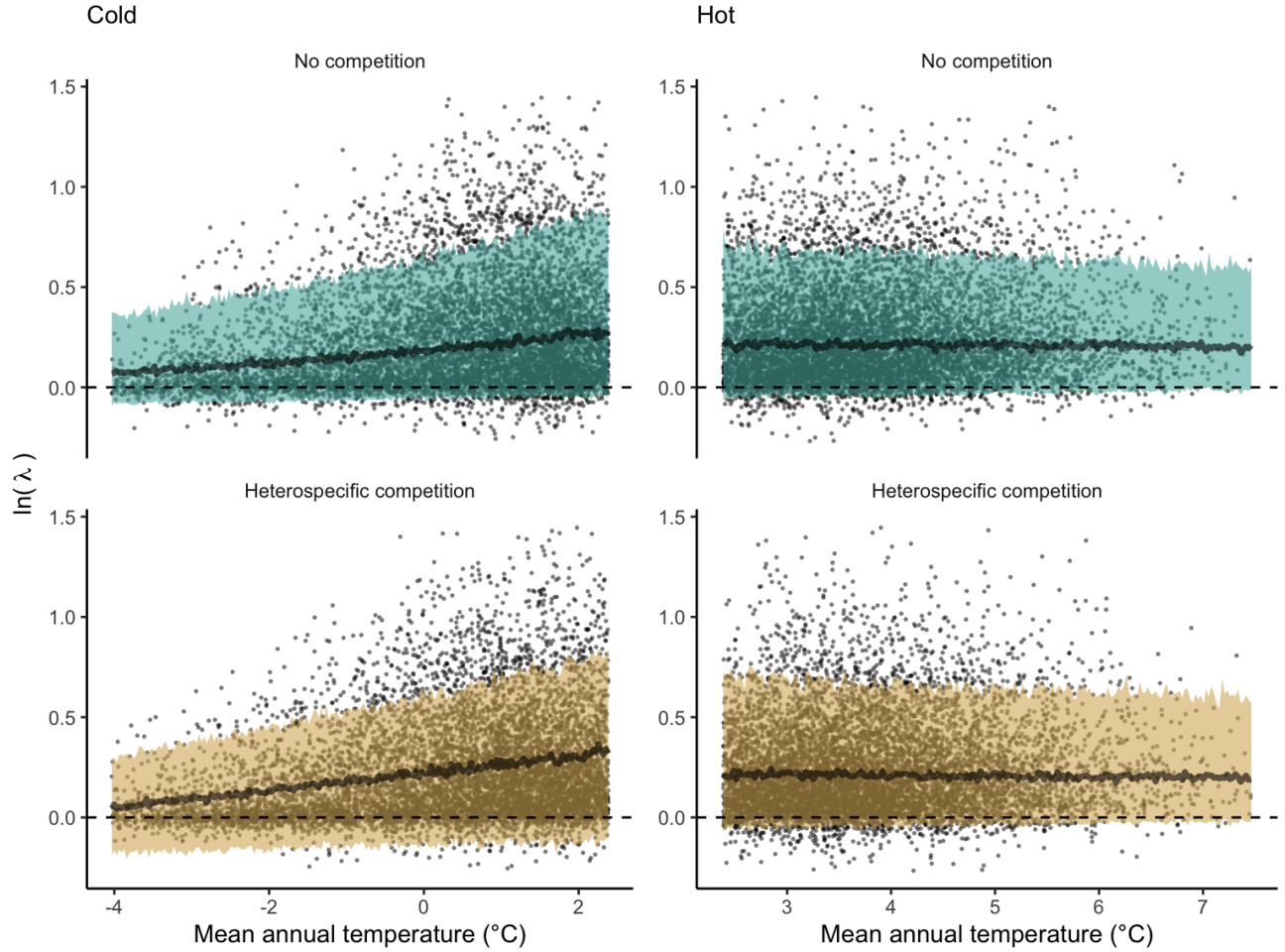


Figure 1: Distribution of stochastic population growth rate (λ) for *Abies balsamea* over the mean annual temperature gradient for cold (left panels) and hot (right panels) ranges under no competition (fundamental niche) and heterospecific competition (realized niche). The dots represent λ over the plot-year-replication combinations. The model's average line and 90% prediction intervals are estimated using 500 draws from the posterior distribution.

278 We then investigated the local suitability probability using the empirical cumulative distribution approach
 279 (Equation 4) from the linear model predictions. The Figure 2 shows the suitable probability expected
 280 over the mean annual temperature of the same species. We observed that the local suitability probability

was reduced towards the cold border, with a stronger reduction under heterospecific competition (yellow curve). We can also observe that the decrease in suitable probability towards the border is nonlinear, becoming more substantial for heterospecific competition than for the no-competition condition.

The model fit and the estimation of suitable probability across the temperature gradient for all species are presented in Supplementary Material 2. We observed for most species a decrease of the climate effect at one border while the other remained unchanged. Additionally, a few species displayed a clear linear pattern of decreasing suitable probability from the cold to the hot border, with only one species (*Betula papyrifera*) having a decrease at both borders. Conversely, under the competition effect, most species exhibited a decrease in suitable probability at the hot border and an increase at the cold border, indicating a linear rise in the impact of competition from the cold to the hot border of the distribution.

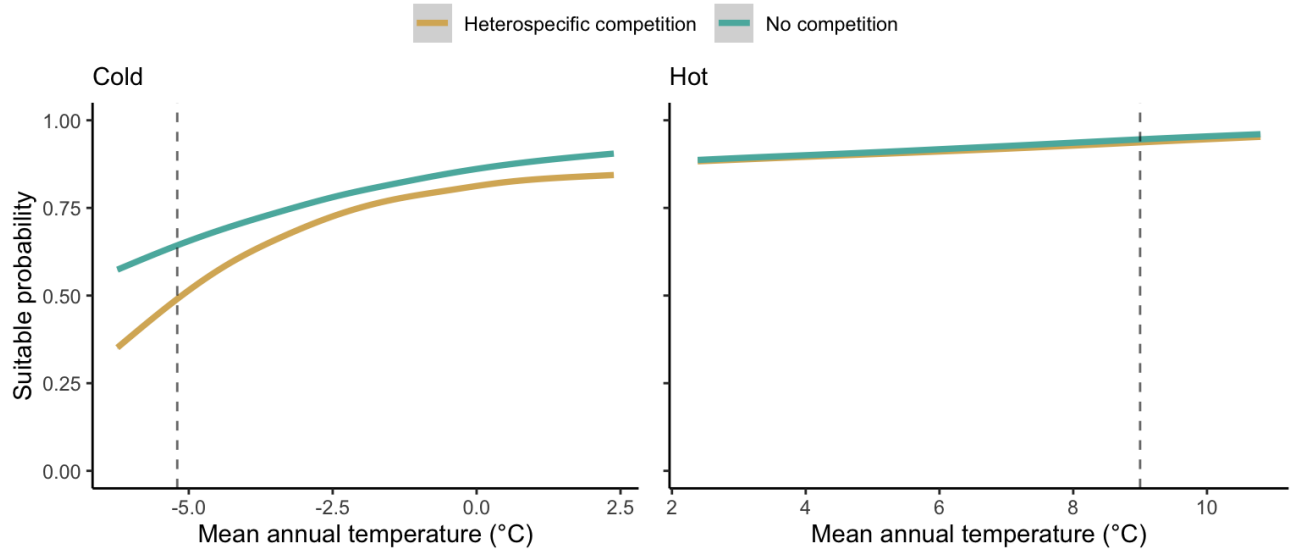


Figure 2: Suitable probability of *Abies balsamea* over the mean annual temperature gradient for cold and hot ranges under no competition (green) and heterospecific (yellow). The vertical dotted line represents the range limits of the MAT observed in the dataset.

3.0.2 Effect of climate and competition on suitable probability for the center and border distributions

We investigated the effect of climate and competition on the suitable probability at the border and center of the temperature range distribution for all species. Because the border and center positions are relative to each species, we could not represent the continuous trend in suitable probability across the MAT for all 31 species together. Instead, we extracted the local suitable probability with and without

heterospecific competition for four locations across the MAT gradient (Figure 3). Overall, suitable probability was high among the species, with an average of 0.78. Among the four locations, species presented a lower suitable probability at the border of the hot range, with an average of 0.67. Across the temperature range, there is a monotonic decrease in suitable probability from the cold border toward the hot border.

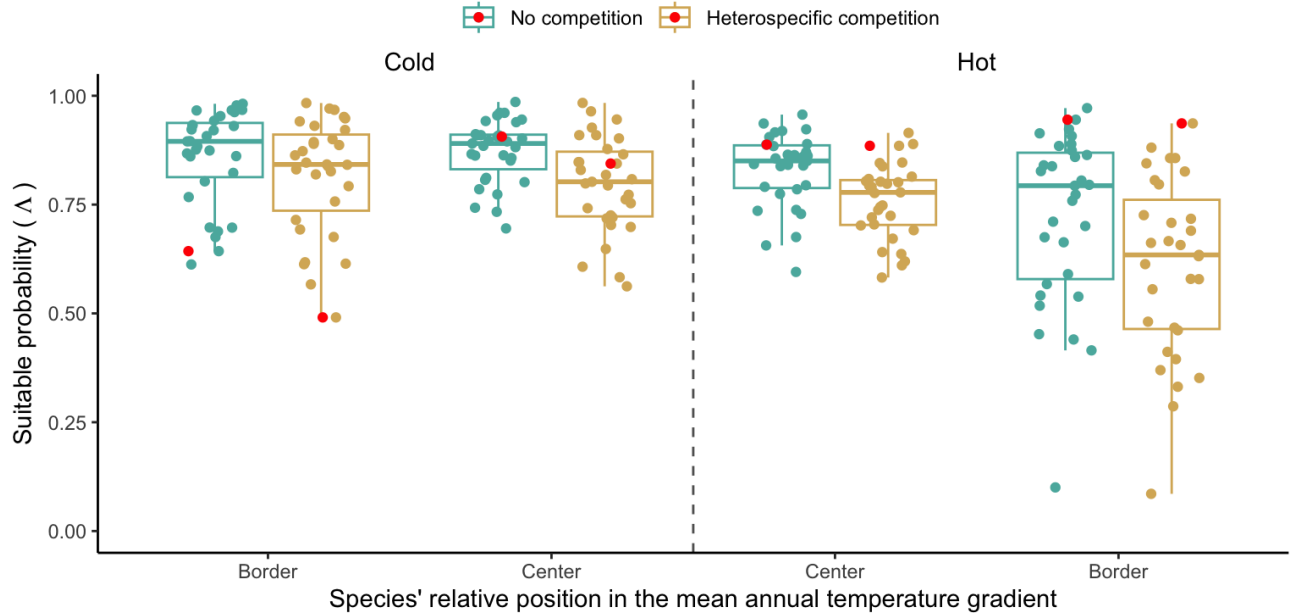


Figure 3: Estimated suitable probability for the 31 forest species across across the center and border of the cold and hot ranges. The x-axis represents the mean annual temperature gradient similar to Figure 2, but is discretized at the border and center limits relative to each species. We highlighted the balsam fir species in red. Note that we omitted the parameter uncertainty of each species in this figure to avoid overlap and increase clarity.

We further disentangle the influence of competition from that of climate by calculating the difference between suitable probability under heterospecific competition and without competition. A negative difference signifies competition reduces suitable probability, while positive differences indicate an increase. Across the four climate locations, heterospecific competition consistently reduced suitable probability for most species, with the magnitude of reduction intensifying from the cold to the hot border (Figure S1). This suggests that the decline in suitable probability observed from the cold to the hot border (Figure 3) results from the combined effect of climate and competition.

3.0.3 Suitable probability change from center to border

We investigated the relative effect of climate and competition on changing suitable probability from the center to the border of the species distribution (Figure 4). A positive relative difference indicates an increase in suitable probability from the center towards the border, while a negative difference indicates a decrease. Most species exhibited a decrease in suitable probability at the hot border relative to the center. Alternatively, most species showed a reduction in the effect of competition toward the cold border. However, the climate effect in the cold range was more variable, with some species experiencing an increase and others a decrease in suitable probability. Overall, the relative difference in suitable probability from the center toward the cold and hot borders was more influenced by climate rather than competition.

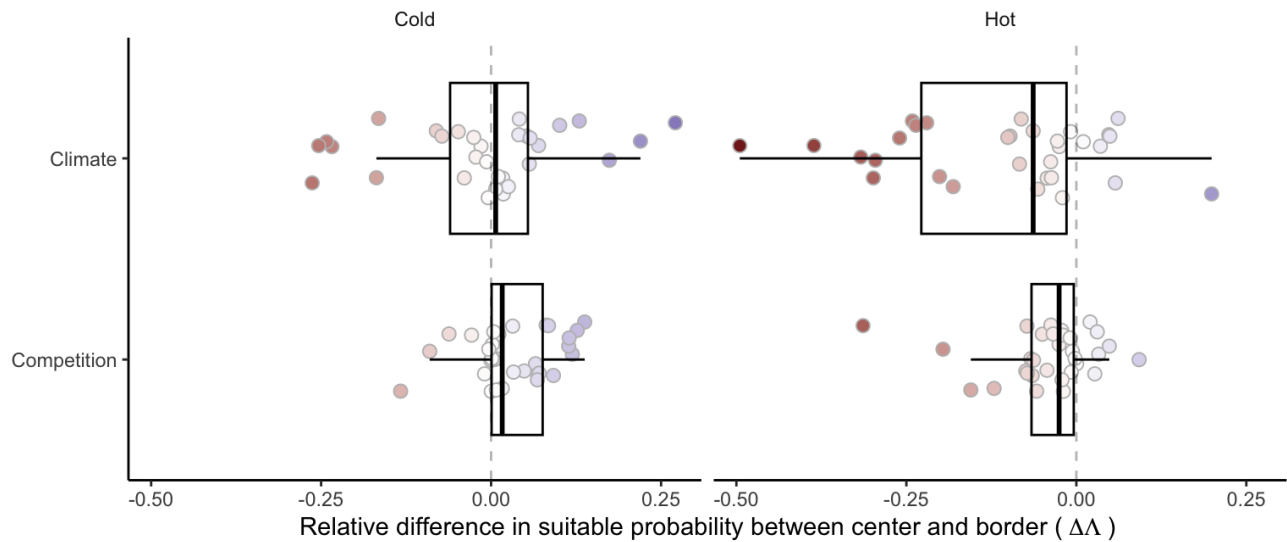


Figure 4: Difference in suitable probability for climate and competition effects over the cold and hot ranges. Negative values denote a decrease in species suitable probability from the center towards the distribution border, while positive values indicate an increase. Specifically, a negative value for climate at the hot (or cold) range signifies a reduction in suitable probability as temperature rises (or falls) towards the border. Boxplots determine the 25-75 quantile distribution among the species.

4 Discussion

Understanding the mechanisms shaping species distribution is imperative to face ongoing global changes. We acknowledged and integrated various sources of variability in the population growth rate of forest

322 trees, contributing to an improved understanding of forest dynamics in an uncertain world. Introducing
323 a novel metric, we quantified the relative impacts of climate and competition on the change in suitable
324 probability across species distributions. Our findings revealed a nearly linear reduction in suitable
325 probability from the cold to hot borders. Notably, the predominant influence on the relative difference in
326 suitable probability from the center toward the border was attributed to climate rather than competition.
327 These results, supported by a novel approach accounting for uncertainty, enhance our understanding of
328 the nuanced interplay between climate and competition across species ranges.

329 The suitable probability was high across all species and range locations, with only around 5% of all
330 species-location combinations having a suitable probability below the 0.5 threshold. This is primarily
331 attributed to most species exhibiting a high positive population growth rate across their current
332 range distribution. Additionally, the spatio-temporal variability in the environment and the parameter
333 uncertainty in the plot may contribute to the elevated average population growth rate due to nonlinear
334 averaging. This aligns with theoretical (Schreiber and Lloyd-Smith 2009) and empirical (Crone 2016)
335 studies suggesting that spatial heterogeneity should increase the population growth rate.

336 Competition significantly reduces local suitability across all range locations, with a stronger and more
337 consistent effect at the cold border, contributing to the ongoing debate surrounding its significance
338 in setting range limits. Despite several studies emphasizing the effect of competition compared to
339 climate on the demographic rates of forest trees (Zhang et al. 2015, Käber et al. 2021, Le Squin et al.
340 2021), debates persist regarding whether this effect at the local scale translates to the biogeographic
341 distribution of species (Soberón 2007, Copenhaver-Parry et al. 2017). Our findings support the Godsoe
342 et al. (2017) hypothesis and a growing body of evidence (Scherrer et al. 2020, Shi et al. 2020, Paquette
343 and Hargreaves 2021, Lyu and Alexander 2022) showing that the effect of competition on the intrinsic
344 population growth rate can indeed contribute to range limits.

345 The decline in suitable probability from the cold to the hot border suggests a predominantly linear,
346 rather than unimodal, relationship with temperature for most species. This result is consistent with
347 reduced population growth rates in North American (Le Squin et al. 2021, Schultz et al. 2022) and
348 European (Guyennon et al. 2023) forest trees, except for the contrasting pattern observation by Purves
349 (2009). The higher suitable probability in the cold range compared to the hot range could be attributed

350 to multiple factors. First, species may still follow their climate niche post the last glaciation, explaining
351 why the current cold range limit does not align with the expected niche distribution (Svenning and
352 Skov 2007), potentially leading to a colonization debt (Talluto et al. 2017). Notably, four of the six
353 species exhibiting a significant decrease in suitable probability from the center toward the cold range
354 were already at the extreme cold observed in the dataset (Figure S4).

355 Our model may however overlook crucial drivers of species performance, despite capturing a substantial
356 amount of variation from parameter uncertainty at the plot level. Factors such as the impact of extreme
357 temperature and precipitation on phenology can influence tree range limits (Morin et al. 2007). Beyond
358 covariates and plot-level uncertainty, incorporating temporal uncertainty at the plot level, accounting
359 for spatio-temporal covariance, could likely capture additional sources of variation in demographic rates.
360 While our approach considers temporal stochasticity in climate and competition, which affect species
361 range size (Holt et al. 2022), there remains temporal variation in demographic rates beyond these
362 covariates. This variability, possibly captured with random effects at the plot level, can influence range
363 limits based on the degree of temporal autocorrelation and its relationship with the range (Benning et
364 al. 2022). For instance, an empirical study on perennial herbaceous species demonstrated that temporal
365 environmental stochasticity reduced the population growth rate relative to the average (Crone 2016).
366 In our study, this temporal variability is particularly relevant for survival (due to disturbance) and
367 recruitment (due to phenology) rates because, in addition to having high temporal variability (Clark et
368 al. 1999, de Souza Leite et al. 2023), they represent the most significant drivers of population growth
369 rate (Chapter 2).

370 The effect of competition, similar to climate, increased from the center towards the border of the hot
371 range, contrary to Kunstler et al. (2021), who found no difference in the competition effect between the
372 center and border of the species. Additionally, our results deviate from the Species Interactions-Abiotic
373 Stress Hypothesis, predicting a stronger competition effect in less stressful climate conditions (Louthan
374 et al. 2015). When considering the relative position of the species across the temperature gradient,
375 only the effect of climate at the cold range changed with temperature. This indicates that most species
376 have a similar or higher suitable probability at the border of the cold range compared to their center
377 distribution. We further tested whether the species' range size affects the relative difference in suitable
378 probability; while the absolute values change, the pattern among the species remains unchanged.

379 The climate gradient of temperature had a more significant effect than competition in changing the
 380 suitable probability of forest trees. This means that mean annual temperature, along with all latent
 381 variables, better explains how suitable probability changes across the temperature range. The choice of
 382 using only mean annual temperature as an explanatory variable for the variance of λ can be improved.
 383 For instance, the model could be built accounting for mean annual temperature and precipitation to
 384 predict the complete two-dimensional distribution of the species' climate niche. Plot random effects
 385 could be further used to account for the nestedness of the data design, allowing the proper separation of
 386 the total variance of the metamodel into variance arising from individual- and plot-level demographic
 387 uncertainty. While we have assumed climate variability as independent and identically distributed
 388 random variables, this assumption can be relaxed to include temporal autocorrelation. Autocorrelated
 389 environmental fluctuation can significantly change a species' range limits due to nonlinear averaging
 390 (Benning et al. 2022, Holt et al. 2022). Lastly, although coexistence theory assumes the abundance of
 391 competitors to be at equilibrium (Chesson 2000), testing this assumption remains practically impossible.

392 Despite the many ways of improving our study, there is a growing body of evidence indicating a mismatch
 393 between performance and occurrence (McGill 2012, Csergo et al. 2017, Bohner and Diez 2020, Le Squin
 394 et al. 2021, Midolo et al. 2021, Guyennon et al. 2023, Thuiller et al. 2014). Our approach can better
 395 capture the nuanced effect of climate and competition along with the spatio-temporal variation in λ ,
 396 yet it was not enough to fully predict tree range limits. Since species distribution is influenced by
 397 processes at multiple scales (McGill 2010, Heffernan et al. 2014), it is challenging to rely on a single
 398 individual-level performance metric to predict it all (Evans et al. 2016). For instance, dispersion plays a
 399 crucial role in changing species distribution at larger spatial scales, either reducing its extent due to
 400 limited dispersal or increasing it through source-sink dynamics (Pulliam 2000). We propose that our
 401 novel metric, local suitable probability, can be a key unifying factor linking local and landscape scales.

402 Forest trees exhibit variation in their frequency of occurrence across distribution gradients, yet their
 403 relative abundance remains consistent when present (Canham and Thomas 2010). Such observation
 404 implies that assessing forest distribution should focus on colonization and extinction patch dynamics
 405 rather than local performance (Canham and Murphy 2017). However, instead of restricting models
 406 to either local or large scales, we propose using the local suitable probability to reconcile the local
 407 demographic dynamics with the metapopulation theory. Colonization and extinction processes, as

described by metapopulation theory (Levins 1969), are well-suited for describing the mosaic of forest successional stages at the landscape scale resulting from natural disturbances and succession. However, an implicit assumption is that unoccupied patches are necessarily available for colonization. We relax this assumption and quantify patch availability using the local suitable probability metric (Λ). Take an ensemble of patches (p) where individuals can arrive and establish empty patches through colonization (α), and occupied patches can become empty through extinction (ε): Considering an ensemble of patches (p) where individuals can arrive and establish in empty patches through colonization (α), and occupied patches can become empty through extinction (ε), the integrated metapopulation model becomes:

$$\frac{dp}{dt} = \alpha p(\Lambda - p) - \varepsilon p$$

With this formulation, rather than having $1 - p$ available patches for colonization, we have $\Lambda - p$. Therefore, when λ and its variability are high, the local suitable probability equals 1, indicating that all non-occupied patches are available. Conversely, as the local suitable probability decreases, the proportion of non-occupied patches available for colonization is reduced. This integrative approach allows one to account for both the local (e.g. competition and climate) and landscape (e.g. fire disturbances and dispersal) drivers of forest dynamics when assessing tree distribution.

References

- Benning, J. W., R. A. Hufbauer, and C. Weiss-Lehman. 2022. Increasing temporal variance leads to stable species range limits. *Proceedings of the Royal Society B: Biological Sciences* 289.
- Bohner, T., and J. Diez. 2020. Extensive mismatches between species distributions and performance and their relationship to functional traits. *Ecology Letters* 23:33–44.
- Canham, C. D., and L. Murphy. 2017. The demography of tree species response to climate: Sapling and canopy tree survival. *Ecosphere* 8.
- Canham, C. D., and R. Q. Thomas. 2010. Frequency, not relative abundance, of temperate tree species varies along climate gradients in eastern North America. *Ecology* 91:3433–3440.

431 Caswell, H. 2009. Stage, age and individual stochasticity in demography. *Oikos* 118:1763–1782.

432 Chesson, P. 2000. Mechanisms of maintenance of species diversity. *Annu. Rev. Ecol. Syst* 31:343–66.

433 Clark, J. S. 2010. Individuals and the variation needed for high species diversity in forest trees. *Science*
434 327:1129–1132.

435 Clark, J. S., B. Beckage, P. Camill, B. Cleveland, J. HilleRisLambers, J. Lichter, J. McLachlan, J.
436 Mohan, and P. Wyckoff. 1999. Interpreting recruitment limitation in forests. *American Journal of*
437 *Botany* 86:1–16.

438 Copenhaver-Parry, P. E., B. N. Shuman, and D. B. Tinker. 2017. Toward an improved conceptual
439 understanding of North American tree species distributions. *Ecosphere* 8:e01853.

440 Cressie, N., C. A. Calder, J. S. Clark, J. M. Ver Hoef, and C. K. Wikle. 2009. Accounting for uncertainty
441 in ecological analysis: The strengths and limitations of hierarchical statistical modeling. *Ecological*
442 *Applications* 19:553–570.

443 Crone, E. E. 2016. Contrasting effects of spatial heterogeneity and environmental stochasticity on
444 population dynamics of a perennial wildflower. *Journal of Ecology* 104:281–291.

445 Csergo, A. M., R. Salguero-Gómez, O. Broennimann, S. R. Coutts, A. Guisan, A. L. Angert, E. Welk, I.
446 Stott, B. J. Enquist, B. McGill, J.-C. Svenning, C. Violle, and Y. M. Buckley. 2017. Less favourable
447 climates constrain demographic strategies in plants. *Ecology Letters*.

448 Damgaard, C. 2020. Measurement Uncertainty in Ecological and Environmental Models. *Trends in*
449 *Ecology and Evolution* 35:871–873.

450 de Souza Leite, M., S. M. McMahon, P. I. Prado, S. J. Davies, A. A. de Oliveira, H. P. D. Deurwaerder,
451 S. Aguilar, K. J. Anderson-Teixeira, N. Aqilah, N. A. Bourg, W. Y. Brockelman, N. Castaño, C.-H.
452 Chang-Yang, Y.-Y. Chen, G. Chuyong, K. Clay, Álvaro Duque, S. Ediriweera, C. E. N. Ewango,
453 G. Gilbert, I. A. U. N. Gunatilleke, C. V. S. Gunatilleke, R. Howe, W. H. Huasco, A. Itoh, D. J.
454 Johnson, D. Kenfack, K. Král, Y. T. Leong, J. A. Lutz, J.-R. Makana, Y. Malhi, W. J. McShea,
455 M. Mohamad, M. Nasardin, A. Nathalang, G. Parker, R. Parmigiani, R. Pérez, R. P. Phillips, P.

456 Šamonil, I.-F. Sun, S. Tan, D. Thomas, J. Thompson, M. Uriarte, A. Wolf, J. Zimmerman, D. Zuleta,
 457 M. D. Visser, and L. Hülsmann. 2023. Major axes of variation in tree demography across global
 458 forests. *bioRxiv*.

459 Ellner, S. P., D. Z. Childs, and M. Rees. 2016. Data-driven modelling of structured populations.
 460 Springer.

461 Ettinger, A., and J. HilleRisLambers. 2017. Competition and facilitation may lead to asymmetric range
 462 shift dynamics with climate change. *Global Change Biology* 23:3921–3933.

463 Evans, M. E. K., C. Merow, S. Record, S. M. McMahon, and B. J. Enquist. 2016. Towards Process-based
 464 Range Modeling of Many Species. *Trends in Ecology and Evolution* 31:860–871.

465 Gabry, J., R. Češnovar, and A. Johnson. 2023. *cmdstanr*: R Interface to 'CmdStan'.

466 Godsoe, W., J. Jankowski, R. D. Holt, and D. Gravel. 2017. Integrating Biogeography with Contempo-
 467 rary Niche Theory. *Trends in Ecology and Evolution* 32:488–499.

468 Gravel, D., F. Guichard, and M. E. Hochberg. 2011. Species coexistence in a variable world. *Ecology*
 469 *Letters* 14:828–839.

470 Guyennon, A., B. Reineking, R. Salguero-Gomez, J. Dahlgren, A. Lehtonen, S. Ratcliffe, P. Ruiz-Benito,
 471 M. A. Zavala, and G. Kunstler. 2023. Beyond mean fitness: Demographic stochasticity and resilience
 472 matter at tree species climatic edges. *Global Ecology and Biogeography* 32:573–585.

473 Harwood, J., and K. Stokes. 2003. Coping with uncertainty in ecological advice: Lessons from fisheries.
 474 *Trends in Ecology and Evolution* 18:617–622.

475 Heffernan, J. B., P. A. Soranno, M. J. Angilletta, L. B. Buckley, D. S. Gruner, T. H. Keitt, J. R. Kellner,
 476 J. S. Kominoski, A. V. Rocha, and J. Xiao. 2014. Macrosystems ecology: understanding ecological
 477 patterns and processes at continental scales. *Frontiers in Ecology and the Environment* 12:5–14.

478 Holt, R. D. 2009. Bringing the Hutchinsonian niche into the 21st century: ecological and evolutionary
 479 perspectives. *Proceedings of the National Academy of Sciences* 106:19659–19665.

480 Holt, R. D., M. Barfield, and J. H. Peniston. 2022. Temporal variation may have diverse impacts on
481 range limits. *Philosophical Transactions of the Royal Society B: Biological Sciences* 377.

482 Holt, R. D., T. H. Keitt, M. a Lewis, B. a Maurer, and M. L. Taper. 2005. Theoretical models of
483 species' borders: single species approaches. *Schurr*2012 108:18–27.

484 Hutchinson, G. E. 1957. Concluding remarks. Pages 415–427 *in* Cold spring harbor symposium on
485 quantitative biology.

486 Käber, Y., P. Meyer, J. Stillhard, E. De Lombaerde, J. Zell, G. Stadelmann, H. Bugmann, and C. Bigler.
487 2021. Tree recruitment is determined by stand structure and shade tolerance with uncertain role of
488 climate and water relations. *Ecology and Evolution* 11:12182–12203.

489 Koons, D. N., S. Pavard, A. Baudisch, and C. Jessica E. Metcalf. 2009. Is life-history buffering or
490 lability adaptive in stochastic environments? *Oikos* 118:972–980.

491 Kunstler, G., A. Guyennon, S. Ratcliffe, N. Rüger, P. Ruiz-Benito, D. Z. Childs, J. Dahlgren, A.
492 Lehtonen, W. Thuiller, C. Wirth, M. A. Zavala, and R. Salguero-Gomez. 2021. Demographic
493 performance of European tree species at their hot and cold climatic edges. *Journal of Ecology*
494 109:1041–1054.

495 Leslie, P. H. 1945. On the use of matrices in certain population mathematics. *Sankhyt* 33:183–212.

496 Le Squin, A., I. Boulangeat, and D. Gravel. 2021. Climate-induced variation in the demography of 14
497 tree species is not sufficient to explain their distribution in eastern North America. *Global Ecology*
498 *and Biogeography* 30:352–369.

499 Levins, R. 1969. Some Demographic and Genetic Consequences of Environmental Heterogeneity for
500 Biological Control. *Bulletin of the Entomological Society of America* 15:237–240.

501 Lewis, E. G. 1942. On the generation and growth of a population. *Sankhyā* 6:93–96.

502 Louthan, A. M., D. F. Doak, and A. L. Angert. 2015. Where and When do Species Interactions Set
503 Range Limits? *Trends in Ecology and Evolution* 30:780–792.

504 Lyu, S., and J. M. Alexander. 2022. Competition contributes to both warm and cool range edges.
505 Nature Communications 13:1–9.

506 Maguire Jr, B. 1973. Niche response structure and the analytical potentials of its relationship to the
507 habitat. The American Naturalist 107:213–246.

508 May, R. M., J. R. Beddington, J. W. Horwood, and J. G. Shepherd. 1978. Exploiting natural populations
509 in an uncertain world. Mathematical Biosciences 42:219–252.

510 McGill, B. J. 2010. Matters of scale. Science 328:575–576.

511 McGill, B. J. 2012. Trees are rarely most abundant where they grow best. Journal of Plant Ecology
512 5:46–51.

513 Midolo, G., C. Wellstein, and S. Faurby. 2021. Individual fitness is decoupled from coarse-scale
514 probability of occurrence in North American trees. Ecography 44:789–801.

515 Milles, A., T. Banitz, M. Bielcik, K. Frank, C. A. Gallagher, F. Jeltsch, J. U. Jepsen, D. Oro, V.
516 Radchuk, and V. Grimm. 2023. Local buffer mechanisms for population persistence. Trends in
517 Ecology & Evolution 38:1051–1059.

518 Ministère des Ressources Naturelles. 2016. Norme d’inventaire ecoforestier: placettes-echantillons
519 temporaires. Direction des inventaires forestier, Ministère des Ressources naturelles, Québec.

520 Morin, X., C. Augspurger, and I. Chuine. 2007. Process-based modeling of species’ distributions: what
521 limits temperate tree species’ range boundaries? Ecology 88:2280–2291.

522 O’Connell, M. B., E. B. LaPoint, J. A. Turner, T. Ridley, D. Boyer, A. Wilson, K. L. Waddell, and
523 B. L. Conkling. 2007. The forest inventory and analysis database: Database description and users
524 forest inventory and analysis program. US Department of Agriculture, Forest Service.

525 Paquette, A., and A. L. Hargreaves. 2021. Biotic interactions are more often important at species’
526 warm versus cool range edges. Ecology Letters 24:2427–2438.

527 Pulliam, H. R. 2000. On the relationship between niche and distribution. Ecology Letters 3:349–361.

528 Purves, D. W. 2009. The demography of range boundaries versus range cores in eastern US tree species.
529 Proceedings of the Royal Society B: Biological Sciences 276:1477–1484.

530 Scherrer, D., Y. Vitasse, A. Guisan, T. Wohlgemuth, and H. Lischke. 2020. Competition and demography
531 rather than dispersal limitation slow down upward shifts of trees’ upper elevation limits in the Alps.
532 Journal of Ecology:1–15.

533 Schreiber, S. J., and J. O. Lloyd-Smith. 2009. Invasion dynamics in spatially heterogeneous environments.
534 American Naturalist 174:490–505.

535 Schultz, E. L., L. Hülsmann, M. D. Pillet, F. Hartig, D. D. Breshears, S. Record, J. D. Shaw, R. J.
536 DeRose, P. A. Zuidema, and M. E. K. Evans. 2022. Climate-driven, but dynamic and complex? A
537 reconciliation of competing hypotheses for species’ distributions. Ecology letters 25:38–51.

538 Shi, H., Q. Zhou, F. Xie, N. He, R. He, K. Zhang, Q. Zhang, and H. Dang. 2020. Disparity in elevational
539 shifts of upper species limits in response to recent climate warming in the Qinling Mountains,
540 North-central China. Science of the Total Environment 706:135718.

541 Shoemaker, L. G., L. L. Sullivan, I. Donohue, J. S. Cabral, R. J. Williams, M. M. Mayfield, J. M. Chase,
542 C. Chu, W. S. Harpole, A. Huth, J. HilleRisLambers, A. R. M. James, N. J. B. Kraft, F. May, R.
543 Muthukrishnan, S. Satterlee, F. Taubert, X. Wang, T. Wiegand, Q. Yang, and K. C. Abbott. 2020.
544 Integrating the underlying structure of stochasticity into community ecology. Ecology 101:1–15.

545 Sittaro, F., A. Paquette, C. Messier, and C. A. Nock. 2017. Tree range expansion in eastern North
546 America fails to keep pace with climate warming at northern range limits. Global Change Biology:1–
547 10.

548 Soberón, J. 2007. Grinnellian and Eltonian niches and geographic distributions of species. Ecology
549 Letters 10:1115–1123.

550 Svenning, J. C., and F. Skov. 2007. Could the tree diversity pattern in Europe be generated by
551 postglacial dispersal limitation? Ecology Letters 10:453–460.

552 Talluto, M. V., I. Boulangeat, S. Vissault, W. Thuiller, and D. Gravel. 2017. Extinction debt and

553 colonization credit delay range shifts of eastern North American trees. *Nature Ecology & Evolution*
554 1:0182.

555 Team, S. D., and Others. 2022. Stan modeling language users guide and reference manual, version
556 2.30.1. Stan Development Team.

557 Terry, J. C. D., J. D. O’Sullivan, and A. G. Rossberg. 2022. Synthesising the multiple impacts of
558 climatic variability on community responses to climate change. *Ecography* 2022:e06123.

559 Thuiller, W., T. Munkemuller, K. H. Schiffers, D. Georges, S. Dullinger, V. M. Eckhart, T. C. Edwards,
560 D. Gravel, G. Kunstler, C. Merow, K. Moore, C. Piedallu, S. Vissault, N. E. Zimmermann, D. Zurell,
561 F. M. Schurr, T. Münkemüller, K. H. Schiffers, D. Georges, S. Dullinger, V. M. Eckhart, T. C.
562 Edwards, D. Gravel, G. Kunstler, C. Merow, K. Moore, C. Piedallu, S. Vissault, N. E. Zimmermann,
563 D. Zurell, and F. M. Schurr. 2014. Does probability of occurrence relate to population dynamics?
564 *Ecography* 37:1155–1166.

565 van Daalen, S., and H. Caswell. 2020. Variance as a life history outcome: Sensitivity analysis of the
566 contributions of stochasticity and heterogeneity. *Ecological Modelling* 417.

567 Zhang, J., S. Huang, and F. He. 2015. Half-century evidence from western Canada shows forest
568 dynamics are primarily driven by competition followed by climate. *Proceedings of the National*
569 Academy of Sciences 112:4009–4014.